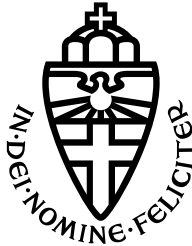


RADBOUD UNIVERSITY NIJMEGEN



INSTITUTE FOR MATHEMATICS, ASTROPHYSICS AND PARTICLE PHYSICS  
DEPARTMENT OF HIGH ENERGY PHYSICS

---

# Late universe neutrino creation in a curvature dependent dark energy model

EXPLORING IF A CURVATURE DEPENDENT DARK ENERGY MODEL WITH  
NEUTRINO CREATION CAN EXPLAIN DARK MATTER AND ITS IMPLICATIONS  
FOR COSMIC NEUTRINO BACKGROUND MEASUREMENTS

---

THESIS BSc PHYSICS AND ASTRONOMY  
April 2024

*Author:*  
Jesse Cools

*Supervisor:*  
Prof. Dr. W.J.P. Beenakker

*Second reader:*  
Prof. Dr. N. de Groot

## Acknowledgements

I would like to thank everyone who helped me in the process of creating this bachelors thesis. First of all I would like to thank my supervisor Wim Beenakker. Throughout the process of writing this thesis, he has taught me to think and research critically, and has helped me tremendously whenever I was unsure about how to progress in this project. Second of all I would like to thank Tijmen Melssen, for helping me get used to this subject, being an invaluable resource while researching and writing this thesis and improving my morale by accompanying me when restocking our coffee and water and cracking jokes together more times than I can count. I would like to thank my predecessors Bas van den Hoek and Thijs van Rossum, for helping me get to know the subject and laying the groundwork for my thesis. I would like to thank Berend Coenen. His cooked food and presence always helped replenish a significant amount of the energy expended by researching and writing. Lastly I would like to thank all family and friends. Their support has, probably unbeknownst to them, been an amazing source of help while writing this thesis. I will end this section by saying that everyone mentioned above has made writing this thesis orders of magnitude easier and I could not be more thankful.

# Contents

<b>1</b>	<b>Introduction to cosmology</b>	<b>3</b>
<b>2</b>	<b>Conventions</b>	<b>5</b>
<b>3</b>	<b><math>\Lambda</math>-CDM</b>	<b>6</b>
3.1	Stress-energy tensor . . . . .	7
<b>4</b>	<b>Curvature Dependent Dark Energy model</b>	<b>10</b>
4.1	Effect on the Einstein equations . . . . .	10
4.2	CDDE model . . . . .	10
4.3	Matter creation . . . . .	11
<b>5</b>	<b>Phase space density</b>	<b>14</b>
5.1	Dark matter halos . . . . .	14
5.2	Fine grained . . . . .	15
5.3	Coarse grained . . . . .	15
<b>6</b>	<b>CNB temperature</b>	<b>20</b>
6.1	Introduction to the CNB . . . . .	20
6.2	CNB pressure and energy density . . . . .	20
6.3	CNB temperature and number density . . . . .	24
<b>7</b>	<b>Filling the universe and CNB noise</b>	<b>26</b>
7.1	Filling the universe . . . . .	26
7.2	CNB noise . . . . .	27
7.2.1	Inverted hierarchy . . . . .	28
7.2.2	Normal hierarchy . . . . .	29
<b>8</b>	<b>Outlook and conclusions</b>	<b>31</b>
<b>A</b>	<b>Jeans equations for an isothermal density profile.</b>	<b>32</b>

# 1 Introduction to cosmology

In 1915 Einstein published his theory of general relativity. This theory described a model for gravity in which the famous Einstein field equations described the impact of matter, and other forms of energy, momenta and different forms of stress on the curvature of spacetime. These equations are given below:

$$R_{\mu\nu} - \frac{1}{2}g_{\mu\nu}R = 8\pi GT_{\mu\nu}^{\text{eff}}. \quad (1.1)$$

In these equations  $R_{\mu\nu}$  denotes the Ricci tensor,  $g_{\mu\nu}$  the metric of the system,  $R$  the Ricci scalar,  $G$  Newton's gravitational constant and  $T_{\mu\nu}^{\text{eff}}$  the effective stress energy tensor. These equations are a very important tool for cosmologists to model the current and past universe.

Another important concept for cosmology is the scale factor  $a(t)$ . This is a very useful quantity when talking about the expansion of the universe. The scale factor is defined by the following formula:

$$d(t) = a(t)d_0 \quad (1.2)$$

where  $d(t)$  is the proper distance between two objects at time  $t$  and  $d_0$  is the proper distance between these two objects at a reference time  $t_0$ . It is convention to choose  $t_0$  as the current time and setting  $t = 0$  at the big bang. This automatically implies that  $t_0$  is equal to the age of the universe. From these conventions and equation 1.2 it follows that  $a(t_0) = 1$ . If light travels through an expanding universe, its wavelength gets expanded by a factor  $1 + z$ , which for visible light shifts it towards the red part of the light spectrum. This is called redshift. The redshift  $z$  and the scale factor are inversely related by:

$$z = \frac{1}{a(t)} - 1, \quad a(t) = \frac{1}{1 + z}. \quad (1.3)$$

The convention in cosmology is to use redshift as a time parameter, since it is easily measurable, and it has a simple relation to the scale factor, so this will also be used in this thesis. Another very important concept in cosmology is the Hubble parameter  $H(t)$ . This parameter describes the proportionality between the proper distance between two objects, and their recessional velocity, which is the velocity due to the expansion of the universe. The scale factor can be used to calculate the Hubble parameter with the following formula:

$$H = \frac{\dot{a}(t)}{a(t)} = \frac{1}{a(t)} \frac{d}{dt} a(t). \quad (1.4)$$

The Hubble constant  $H_0$  is the value of the Hubble parameter at the current time  $H_0 = H(t_0)$ . The Hubble parameter is usually expressed in kilometers per second per megaparsec, so a Hubble parameter with a value of 1 will mean that two objects with a proper distance of one megaparsec will have a velocity of 1

km/s relative to each other. The Hubble parameter can be measured in multiple ways, for example by looking at galaxies and determining their redshift. This redshift has to be corrected for so called "peculiar motion". This entails velocity shifts due to gravitational effects, such as galaxies being gravitationally affected by other galaxies inside a cluster. These effects are accounted for by modelling these gravitational effects to find out what corrections have to be made to the measured redshift. The calculated corrected redshift of these objects would make it possible to calculate the Hubble parameter if the distance to these objects is known. To measure distances astronomers use cepheid variables, which are stars that vary in brightness in a well-defined periodic way, and type 1a supernovae, which have approximately the same brightness when they collapse and explode after reaching about 1.44 solar masses[1]. The measured luminosity of such a star and its absolute luminosity are then used to calculate its distance to earth. This approach of calculating the Hubble parameter by measuring redshift and distance gives a present-day value (Hubble constant) of  $H_0^{\text{late}} = 73.3 \pm 0.8 \text{ km/s/Mpc}$  [2]. Another way to measure the Hubble constant is by looking at the Cosmic microwave background (CMB). This is a relic from when the photons in the early universe stopped interacting with the subatomic particle plasma, because the universe cooled down enough for neutral atoms to form, which effectively stopped Thomson scattering. It is possible to predict what CMB measurements will look like with your cosmological model and the Hubble parameter. Changing the Hubble constant to match the model's predictions with the measurements then gives us the early universe measurement of the Hubble constant:  $H_0^{\text{early}} = 67.4 \pm 0.5 \text{ km/s/Mpc}$  [2]. It is important to note that this measurement relies on the used model to be correct. This difference between the late and early universe measurements is called the Hubble tension, and can be seen in figure 1.

Since the early universe measurement is model dependent, this tension can be solved by changing the model for the universe. In section 2 we list the relevant conventions. In section 3 we will explain how the current model works, then in section 4 we will explain our model of the universe, which solves the Hubble tension. Our model has some interesting properties like matter creation. This created matter will probably consist of neutrinos, so in section 5 I will be looking at the implications of this neutrino creation on dark matter halos and in sections 6 and 7 at its effect on the cosmic neutrino background.

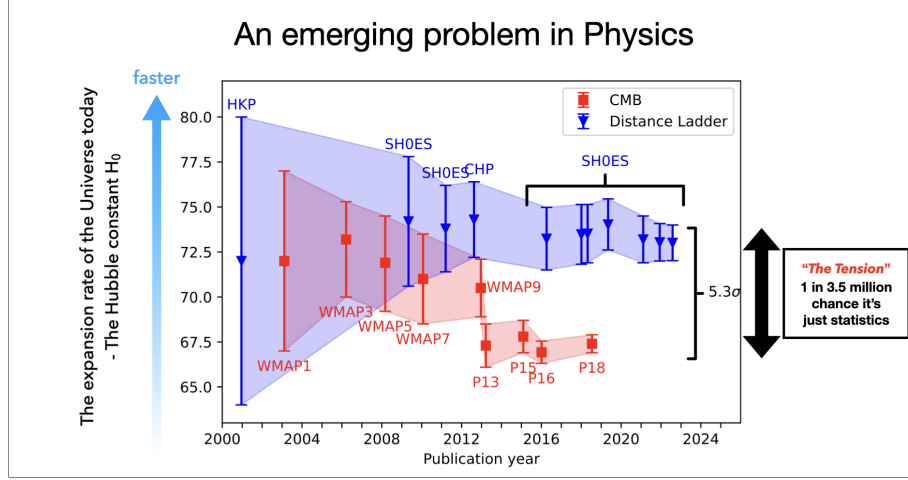


Figure 1: A graph showing the evolving tension between the late and early universe measurements over the years. It can be seen that as the years progressed, the probability of the tension being caused by measurement uncertainties decreased significantly. Taken from [3]

## 2 Conventions

Here is a short overview of the used conventions, to make it clear what is meant by certain notations in the rest of the thesis.

We make use of natural units, which means that unless otherwise stated:

$$c = \hbar = 1 \quad (2.1)$$

We make use of Newton's dot notation for time derivatives:

$$\dot{a}(t) = \frac{d}{dt}a(t), \quad \ddot{a}(t) = \frac{d^2}{dt^2}a(t) \quad (2.2)$$

When using 4-vectors and tensors, the Einstein summation convention is used, which means we sum over repeated indices:

$$a_\mu x^\mu = a_0 x^0 + a_1 x^1 + a_2 x^2 + a_3 x^3. \quad (2.3)$$

The correct hierarchy of neutrino mass eigenstates is currently unknown. We will denote the three light neutrino mass eigenstates by  $\nu_i$ , with  $i = 1, 2, 3$ . These will denote the mass eigenstates in ascending order of mass. It is important to remember that this means that the lightest neutrino mass eigenstate  $\nu_1$ , will not have the same flavour components (labeled  $\nu_e, \nu_\mu, \nu_\tau$ ) in the so called "normal hierarchy", as in the "inverted hierarchy". A graphical representation of this is shown below:

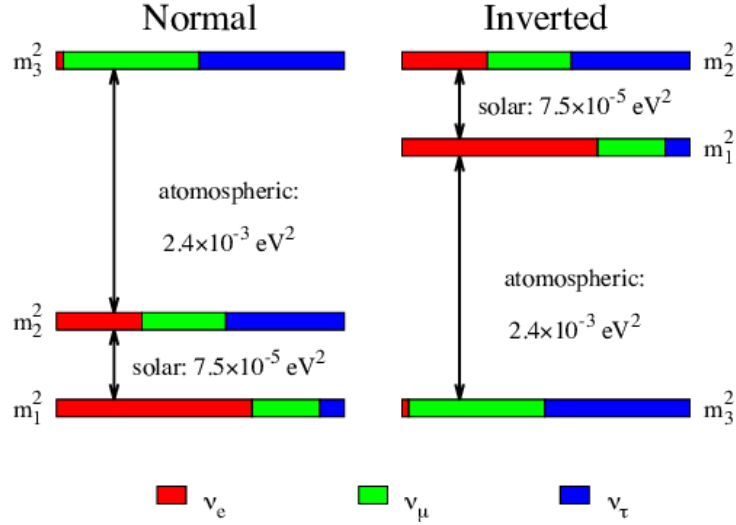


Figure 2: A figure showing the relation between mass and flavour eigenstates of the light neutrinos in the normal and inverted hierarchy. Taken from [4]

### 3 $\Lambda$ -CDM

The standard cosmological model used in the determination of the Hubble parameter is called the Lambda-Cold Dark Matter ( $\Lambda$ -CDM) model. The Lambda refers to the cosmological constant present in this model. The cold dark matter is matter that is non-baryonic, that is non-relativistic when radiation and matter were equal in the universe, that cannot cool by radiating photons and that only interacts with other particles by gravity and possibly a weak force. The  $\Lambda$ -CDM model assumes large scale isotropy and homogeneity which is supported by [5] for scales larger than around 100 Mpc. The Einstein equations in this model look like:

$$R_{\mu\nu} - \frac{1}{2}g_{\mu\nu}R = 8\pi GT_{\mu\nu}^{\text{eff}}, \quad \text{where} \quad T_{\mu\nu}^{\text{eff}} = T_{\mu\nu}^{\text{mat}} + \frac{\Lambda}{8\pi G}g_{\mu\nu}. \quad (3.1)$$

Here  $\Lambda$  is the cosmological constant this model is named after, and  $T_{\mu\nu}^{\text{mat}}$  is the part of the stress-energy tensor containing all contributions by matter and radiation. This model uses the Friedmann–Lemaître–Robertson–Walker metric which is given by

$$g_{\mu\nu}^{\text{FRW}} = \text{diag} \left( 1, -\frac{a^2(t)}{1 - \kappa r^2}, -a^2(t)r^2, -a^2(t)r^2 \sin^2(\theta) \right) \quad (3.2)$$

in spherical coordinates. In this equation we have used natural units ( $c=1$ ) and  $\kappa$  denotes the intrinsic spatial curvature of the universe. Results from the Planck collaboration [6] are in agreement with a spatially flat universe, so we

will set  $\kappa$  to 0 in our model. This reduces our metric to:

$$g_{\mu\nu}^{\text{FRW}} = \text{diag} (1, -a^2(t), -a^2(t)r^2, -a^2(t)r^2 \sin^2(\theta)). \quad (3.3)$$

Having now obtained our metric, it is possible to calculate the Christoffel symbols needed for the calculation of the Ricci tensor and Ricci scalar. The Christoffel symbols are calculated from the metric by:

$$\Gamma_{\nu\rho}^{\mu} = \frac{1}{2}g^{\mu\sigma} (\partial_{\nu}g_{\sigma\rho} + \partial_{\rho}g_{\nu\sigma} - \partial_{\sigma}g_{\nu\rho}). \quad (3.4)$$

Here  $g^{\mu\sigma}$  denotes the inverse metric and  $\partial_{\nu}$  denotes the partial derivative with respect to  $x^{\nu}$ . The non-zero Christoffel symbols for the metric are given below with  $a \equiv a(t)$ :

$$\begin{aligned} \Gamma_{rr}^t &= a\dot{a} & \Gamma_{\theta\theta}^t &= r^2 a\dot{a} & \Gamma_{\phi\phi}^t &= r^2 \sin^2(\theta) a\dot{a} \\ \Gamma_{tr}^r &= \Gamma_{t\theta}^{\theta} = \Gamma_{t\phi}^{\phi} = \frac{\dot{a}}{a} & \Gamma_{\theta\theta}^r &= -r & \Gamma_{\phi\phi}^r &= -r \sin^2(\theta) \\ \Gamma_{r\theta}^{\theta} &= \frac{1}{r} & \Gamma_{\phi\phi}^{\theta} &= -\cos(\theta) \sin(\theta) \\ \Gamma_{r\phi}^{\phi} &= \frac{1}{r} & \Gamma_{\phi\theta}^{\phi} &= \cot(\theta). \end{aligned} \quad (3.5)$$

All Christoffel symbols are symmetric in their lower indices, so Christoffel symbols with interchanged lower indices have not been written down. The Riemann curvature tensor can then be calculated as follows:

$$R_{\mu\nu\rho}^{\sigma} = \partial_{\nu}\Gamma_{\mu\rho}^{\sigma} - \partial_{\rho}\Gamma_{\mu\nu}^{\sigma} + \Gamma_{\mu\rho}^{\alpha}\Gamma_{\alpha\nu}^{\sigma} - \Gamma_{\mu\nu}^{\alpha}\Gamma_{\alpha\rho}^{\sigma}. \quad (3.6)$$

The Riemann curvature tensor makes it possible to calculate the Ricci tensor:

$$R_{\mu\rho} = R_{\mu\nu\rho}^{\nu}. \quad (3.7)$$

The non-zero components of the Ricci tensor will then be equal to:

$$R_{00} = -3\frac{\ddot{a}}{a} \quad (3.8)$$

$$R_{\mu\nu} = -\left(\frac{\ddot{a}}{a} + 2\frac{\dot{a}^2}{a^2}\right)g_{\mu\nu}^{\text{FRW}}, \quad \mu = \nu \neq 0 \quad (3.9)$$

We can then calculate the Ricci scalar as:

$$R = g^{\mu\rho}R_{\mu\rho} = -6\left(\frac{\ddot{a}}{a} + \frac{\dot{a}^2}{a^2}\right). \quad (3.10)$$

### 3.1 Stress-energy tensor

The only missing part in Einstein's equations of gravity is the stress-energy tensor. This tensor describes the density and flux of energy and momentum



in spacetime. The  $\Lambda$ -CDM model uses the perfect fluid approximation, which means we assume negligible viscosity, shear stress and heat conduction. This choice is motivated by the aforementioned assumptions of homogeneity and isotropy. The stress-energy tensor only has diagonal components in a perfect fluid. The 00 component is given by the energy density of all relativistic and non relativistic matter. The other diagonal components are given by the pressure, which leads to a stress energy tensor of the following form:

$$T_{\mu\nu}^{\text{mat}} = \text{diag}(\rho, -Pg_{11}^{\text{FRW}}, -Pg_{22}^{\text{FRW}}, -Pg_{33}^{\text{FRW}}). \quad (3.11)$$

Here  $\rho$  denotes the total energy density, which includes the non relativistic matter component and the relativistic radiation component:  $\rho = \rho_{\text{m}} + \rho_{\text{r}}$ . Here the subscript m indicates the matter component, and the subscript r indicates the radiation component of this density. For non-relativistic particles, the kinetic energy associated with the particles' temperature, which is responsible for the matter contribution to the pressure, is very small compared to the much larger energy density from the mass, i.e.  $\rho_{\text{m}} \gg P_{\text{m}}$ . So the total pressure produced by all types of relativistic and non-relativistic matter is approximately given by just the pressure from radiation. The radiation component of the pressure has the following dependence on the radiation part of the energy density term:  $P = \frac{1}{3}\rho_{\text{r}}$ . This is explained later in this thesis by looking at equation 6.7 and 6.13 in the ultra-relativistic limit. The Einstein equations in the  $\Lambda$ -CDM model lead to the following equations:

$$\dot{\rho}_{\text{m}} + \dot{\rho}_{\text{r}} + \frac{\dot{a}}{a}(3\rho_{\text{m}} + 4\rho_{\text{r}}) = 0, \quad (3.12)$$

$$H^2 \equiv \frac{\dot{a}^2}{a^2} = \frac{8\pi G}{3} \left( \rho_{\text{m}} + \rho_{\text{r}} + \frac{\Lambda}{8\pi G} \right) \Rightarrow \bar{\Omega} \equiv 1 = \Omega_{\text{m}} + \Omega_{\text{r}} + \Omega_{\Lambda}. \quad (3.13)$$

Here  $\Omega_{\text{m}} \equiv \frac{8\pi G}{3H^2}\rho_{\text{m}}$ ,  $\Omega_{\text{r}} \equiv \frac{8\pi G}{3H^2}\rho_{\text{r}}$  and  $\Omega_{\Lambda} \equiv \frac{\Lambda}{3H^2}$  are defined as dimensionless parameters that express the density of the constituent parts. These parameters allow us to get an upper boundary on the parts in this model. In this model it is assumed that matter and radiation do not interact with each other. While matter and radiation do interact in the very early universe, there was a thermal equilibrium between the two [7], which is implied by the observation that the cosmic microwave background is a perfect black body [8]. Since the amount of photons was large enough to ionize the atoms, it is valid to assume that the thermal equilibrium was present before the creation of the CMB. Now being able to describe the photons as a black body photon gas, Tijmen Melssen was able to show in his bachelor thesis that the radiation energy density has a scale factor dependence of [9]:

$$\rho_{\text{r}} \propto a^{-4} \quad (3.14)$$

This means that while the two components do interact in the early universe, it is still possible to split equation 3.12 into two equations, that show the dependency of these energy densities on the scale factor and the redshift:

$$\rho_{\text{m}} = \rho_{\text{m},0}a^{-3} = \rho_{\text{m},0}(1+z)^3 \quad (3.15)$$

$$\rho_r = \rho_{r,0}a^{-4} = \rho_{r,0}(1+z)^4. \quad (3.16)$$

Here  $\rho_{m,0}$  denotes the mass energy density at a redshift of  $z = 0$ , and  $\rho_{r,0}$  denotes its radiation counterpart. These proportionalities make sense, because a fixed amount of mass energy density would change inversely proportional to the volume, which scales with  $a^3$  in three spatial dimensions. The (average) radiation energy density has the same property, but also gets its wavelength stretched in an expanding universe, causing the total radiation energy to scale inversely proportional to the scale factor, which is why the total radiation energy density scales proportional to  $a^{-4}$ .

## 4 Curvature Dependent Dark Energy model

The Hubble tension can be solved by using a different model of the universe. Prof. Dr. W.J.P. Beenakker devised a new model to potentially solve this tension based on the observations in [10]. In this paper it was shown that it is possible to solve the Hubble tension by introducing a dynamical dark energy term, which unlike the  $\Lambda$  in  $\Lambda$ -CDM is not constant with respect to time and may cause matter to not evolve according to  $\rho_m \propto a^{-3}$ .

### 4.1 Effect on the Einstein equations

A toy version of this model introduces a scalar-curvature dependency in the vacuum energy, which turns the vacuum part of the stress-energy tensor into a dynamical dark-energy contribution

$$T_{\mu\nu}^{\text{vac}} = C_\gamma \left( -\frac{R}{6} \right)^\gamma g_{\mu\nu}^{\text{FRW}} \quad (4.1)$$

that changes while the universe expands. Here  $C_\gamma$  denotes a positive proportionality constant with its dimensions depending on  $\gamma$ .  $C_\gamma$  is required to be positive to model the measured accelerated expansion of the late time universe. The prefactor of  $-\frac{1}{6}$  is to get rid of the factor  $-6$  in the Ricci scalar which is seen in equation 3.10. We justify this by being able to control the prefactor with the proportionality constant  $C_\gamma$ . The effective stress-energy tensor is then given by simply adding the vacuum and matter/radiation part:

$$T_{\mu\nu}^{\text{eff}} = \text{diag}(\rho, -Pg_{11}^{\text{FRW}}, -Pg_{22}^{\text{FRW}}, -Pg_{33}^{\text{FRW}}) + C_\gamma \left( -\frac{R}{6} \right)^\gamma g_{\mu\nu}^{\text{FRW}}. \quad (4.2)$$

We can see that if we choose  $\gamma$  to be equal to 0, then our model reduces to the  $\Lambda$ -CDM model, with  $C_\gamma = \frac{\Lambda}{8\pi G}$ .

### 4.2 CDDE model

To solve the Hubble tension, a  $\gamma$  of  $\frac{1}{2}$  was chosen, which we will call the Curvature Dependent Dark Energy model (CDDE). This value for  $\gamma$  was chosen due to the dimension of the Ricci scalar, which is  $\frac{1}{\text{length}^2}$ , which in natural units is proportional to  $\text{eV}^2$ . This means that  $\gamma = \frac{1}{2}$  provides the lowest integer solution for the mass dimension of  $\left(-\frac{R}{6}\right)^\gamma$ , and means that  $C_\gamma$  has units of  $\text{eV}^3$ , since the vacuum part of the stress-energy tensor has units of  $\text{eV}^4$ . Implementing the stress-energy tensor with a  $\gamma$  of  $\frac{1}{2}$  into the 00 component of the Einstein equations gives us:

$$\frac{\dot{a}^2}{a^2} = \frac{8\pi G}{3} \left( \rho + C_{1/2} \left( \frac{\ddot{a}}{a} + \frac{\dot{a}^2}{a^2} \right)^{1/2} \right). \quad (4.3)$$

Calculating the spatial ii components of the Einstein equations and eliminating the vacuum term in these equations by a substitution of equation 4.3 we obtain:

$$\frac{\ddot{a}}{a} = \frac{\dot{a}^2}{a^2} - 4\pi G(\rho + P). \quad (4.4)$$

Combining equations 4.3 and 4.4 we obtain the following equation:

$$\frac{\ddot{a}}{a} = -\frac{4\pi G}{3} \left( \rho + 3P - \beta \pm \sqrt{\beta(\rho - 3P + \beta)} \right). \quad (4.5)$$

In order to clean up this equation we defined the parameter  $\beta \equiv \frac{16\pi G}{3} C_{1/2}^2$ . To find out whether the plus or minus sign is correct, we rewrite the equation in the following form:

$$\frac{\ddot{a}}{a} + \frac{4\pi G}{3}(\rho + 3P) = -\frac{4\pi G}{3} \left( -\beta \pm \sqrt{\beta(\rho - 3P + \beta)} \right) \quad (4.6)$$

We know due to the accelerating expansion of the universe that the left-hand side of the equation has to be larger than 0. We know that  $C_{1/2}$  is positive, so  $\beta$  is also positive by definition. It is then trivial to see that the minus sign is the correct one. This yields our acceleration equation:

$$\frac{\ddot{a}}{a} = -\frac{4\pi G}{3} \left( \rho + 3P - \beta - \sqrt{\beta(\rho - 3P + \beta)} \right). \quad (4.7)$$

If we now combine equations 4.4 and 4.7 and then differentiate with respect to time we obtain:

$$\dot{\rho}_m + \dot{\rho}_r + \frac{\sqrt{\beta}}{4\sqrt{\rho_m + \beta}} \dot{\rho}_m + \frac{\dot{a}}{a} (3\rho_m + 4\rho_r) = 0, \quad (4.8)$$

which alternatively can be expressed in the dimensionless density parameters:

$$\overline{\Omega} \equiv 1 = \Omega_m + \Omega_r + \frac{1}{2}\Omega_\beta \left( 1 + \sqrt{1 + \frac{\Omega_m}{\Omega_\beta}} \right), \quad (4.9)$$

where we now have the new parameter  $\Omega_\beta \equiv \frac{8\pi G}{3H^2} \beta$ . These density parameters make the difference between the equations in the CDDE model and equation 3.13 in the  $\Lambda$ -CDM model very apparent.

### 4.3 Matter creation

In the late universe we know that matter and radiation do not interact. This means we are able to split equation 4.8 into a matter and a radiation part. Integrating both of these components of equation 4.8 gives us the dependence of the matter and radiation energy density on the scale factor.

$$\rho_r = \rho_{r,0} a^{-4}, \quad (4.10)$$

$$\rho_m \left( 1 - \frac{2}{1 + \sqrt{\frac{\rho_m + \beta}{\beta}}} \right)^{\frac{1}{4}} = c_0 a^{-3} \quad (4.11)$$

Here  $c_0$  is a constant that is dependent on  $\rho_{m,0}$ . Comparing this to equations 3.15 and 3.16, we see that the radiation energy density evolves in the same manner as in the  $\Lambda$ -CDM model, but the matter energy density does not. In the late universe we know that the matter energy density is going to become a lot smaller than the dark energy density. This means we can evaluate the limit of small  $\rho_m/\beta$  by using Taylor expansions:

$$\lim_{\rho_m/\beta \rightarrow 0} \rho_m \left( 1 - \frac{2}{1 + \sqrt{\frac{\rho_m + \beta}{\beta}}} \right)^{\frac{1}{4}} \approx \rho_m \left( 1 - \frac{2}{1 + 1 + \frac{\rho_m}{2\beta}} \right)^{\frac{1}{4}} \quad (4.12)$$

Cleaning this equation up a little and using a second Taylor expansion we see that:

$$\lim_{\rho_m/\beta \rightarrow 0} \rho_m \left( 1 - \frac{1}{1 + \frac{\rho_m}{4\beta}} \right)^{\frac{1}{4}} \approx \rho_m \left( 1 - \left( 1 - \frac{\rho_m}{4\beta} \right) \right)^{\frac{1}{4}} = \rho_m \left( \frac{\rho_m}{4\beta} \right)^{\frac{1}{4}} \quad (4.13)$$

Equation 4.11 then gives the following relation between the matter density and the scale factor:

$$\rho_m^{\frac{5}{4}} = c_0 (4\beta)^{\frac{1}{4}} a^{-3} \leftrightarrow \rho_m = c_0^{\frac{4}{5}} (4\beta)^{\frac{1}{5}} a^{-2.4} \quad (4.14)$$

We recall that the proportionality of the matter energy density to the scale factor in the  $\Lambda$ -CDM model is  $a^{-3}$ . This is expected, because an energy density of a fixed amount of total mass energy will change inversely proportional to the volume, which scales with  $a^3$  due to the expansion in three spatial directions. The CDDE model has a slower decrease of the matter energy density, meaning that a fixed amount of total mass energy does not describe the matter energy density in our model, and there must be matter creation!

This conclusion of course begs the question of what this created matter is composed of. Actually there is a quantum mechanical process that allows the creation of matter in curved spacetimes with a *changing metric*[11][12][13]. The dark energy in the CDDE model is dependent on the curvature, and this means that the energy scale of our dark energy will be indicative of what type of matter creation is possible. In order to look at the energy scale of our dark energy term we recall that this term is part of equation 4.9

$$\Omega_m + \Omega_r + \frac{1}{2}\Omega_\beta \left( 1 + \sqrt{1 + \frac{\Omega_m}{\Omega_\beta}} \right) = \Omega_m + \Omega_r + \Omega_{DE}. \quad (4.15)$$

If we then recall that the dimensionless density parameters were defined by  $\Omega_i \equiv \frac{8\pi G}{3H^2} \rho_i$ , the dark energy density will be given by:

$$\rho_{DE} = \frac{1}{2}\Omega_\beta \left( 1 + \sqrt{1 + \frac{\Omega_m}{\Omega_\beta}} \right) \frac{3H^2}{8\pi G} \quad (4.16)$$

The dark energy density here has units of  $\text{Energy}^4$ , so we are actually interested in  $\rho_{\text{DE}}^{\frac{1}{4}}$ . Thijs van Rossum showed in his master thesis that this energy density is in the meV range[14]. He also showed that the amount of extra created matter was equal to 57% of the amount of original matter. We know the created particle has to have mass, because the  $R$  term in our model does not talk to radiation. The only possible particle that can then be made with this energy scale in the Standard Model is the neutrino. We will not discuss exotic particle creation and its consequences in this thesis. Our energy scale implies we will only be able to create light neutrinos and this imposes two major questions which we will try to answer in the following sections. First of all, since neutrinos have the properties of dark matter, we will investigate in section 5 if these produced neutrinos can explain the observed dark matter which is bound to galaxies. Second of all, the CDDE model creates an extra 57% extra matter in the form of neutrinos. If a significant amount of these neutrinos are not bound to galactic halos, then these neutrinos would form some sort of a background radiation. This begs the question of possible interference of the CDDE background neutrinos with the neutrinos of the cosmic neutrino background (CNB). This effect of CDDE neutrinos on the CNB neutrinos will be investigated in sections 6 and 7.

## 5 Phase space density

### 5.1 Dark matter halos

Cosmologists found an unexpected result when looking at the rotational speed of objects in galaxies. The rotational velocity of objects in the outskirts of a galaxy was predicted to diminish with distance from the centre of the galaxy. This would make sense, because at sufficiently large distances an increase in the distance from the centre of the galaxy would decrease the strength of the gravitational effect. This decreased gravitational effect would in turn limit the rotational velocity of anything bound to the galaxy. However, this expected decrease was not measured[15]. At distances beyond the stellar disc of the galaxy the measured rotational velocity would not decrease immediately, but the rotational velocity would decrease significantly more slowly as shown in figure 3.

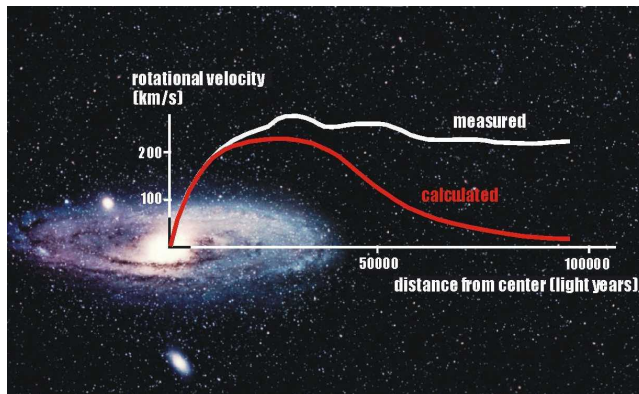


Figure 3: Graph showing the expected and measured values of the rotational velocity as function of distance of objects in a galaxy. Taken from [16]

This result led to the hypothesized existence of a dark matter halo whose particles exist far beyond the observable part of the galaxy. The effects of this halo can also be observed in the movement of individual galaxies in galaxy clusters, gravitational lensing, etc. Dark matter has the properties of not interacting through the electromagnetic force, which means it has a neutral charge. It also only interacts with itself or ordinary matter via gravity and at best a weak force. In his bachelor thesis, Tijmen Melssen showed that (possibly exotic) dark matter was necessary in order to explain the CMB measurements. This dark matter could (partially) consist of the CDDE neutrinos, so we will investigate this possibility in this section.

Investigating the effect of bound CDDE neutrinos is done by looking at different constraints on the phase space in which these neutrinos live. First we take a look at the so called fine grained phase space density. This means looking at the fermions at a microscopic level. Second we look at the so called

coarse grained phase space density which looks at the distribution of neutrinos at a larger scale belonging to gravitational structures. This larger scale is implemented by assuming a continuous mass distribution, which of course does not hold at smaller scales, on which the mass is collected into very small dense regions like stars instead of a continuous density distribution like a gas cloud. This assumption "averages" the density, thus making it a less stringent bound than its fine grained counterpart.

## 5.2 Fine grained

Looking at a Fermi-Dirac distribution it is possible to see that the fine grained momentum phase space number density of relativistic neutrinos is bounded from below in the ultra relativistic limit ( $p \equiv |\vec{p}| \gg m_\nu$ ) by:

$$f_{\text{fg}}(p) = \frac{g_\nu}{h^3} \frac{1}{e^{p/(K_B T)} + 1} \leq \frac{g_\nu}{2h^3}. \quad (5.1)$$

Here  $g_\nu = 4$  for the number of combinations of two spin states and particle or antiparticle for *one* neutrino species,  $K_B$  denotes the Boltzmann constant,  $p$  the momentum and  $T$  the temperature. After the neutrinos decouple, both their energy and temperature decrease proportional to  $1+z$  which implies that the shape of the Fermi-Dirac distribution remains unchanged. The quantity  $f_{\text{fg}}$  describes the number density of neutrinos per unit volume in momentum space, which works well for relativistic neutrinos in view of the direct relation  $E_{\text{kin}} = p$  between kinetic energy (which features in the exponent) and momentum. However when the neutrinos become non-relativistic it is useful to write the phase space density as the mass density of neutrinos per unit volume in velocity space. We will denote this as  $F_{\text{fg}}$ . This will cause an extra factor of  $m_{\nu_i}^3$  from the change of momentum to velocity space in three dimensions, where  $m_{\nu_i}$  denotes the mass of mass eigenstate  $i = 1, 2, 3$  of the neutrino. Changing the number density into a mass density gives another factor  $m_{\nu_i}$ . Swapping the kinetic energy from relativistic to non-relativistic  $E_{\text{kin}} = p \rightarrow E_{\text{kin}} = \frac{1}{2}mv^2 = \frac{p^2}{2m}$  then results in the fine grained non relativistic mass density in velocity phase space:

$$F_{\text{fg}}(v) = \frac{g_\nu m_\nu^4}{h^3} \frac{1}{e^{m_\nu v^2/(2K_B T)} + 1} \leq \frac{g_\nu m_\nu^4}{2h^3}. \quad (5.2)$$

## 5.3 Coarse grained

Our coarse grained phase space density  $F_{\text{cg}}(x, v)$  will describe the phase space density of a finite volume in six dimensional phase space  $\Delta^3 x \Delta^3 v$ . Here we will model the mass density as a continuous mass density to look at gravitational effects, instead of using the very small very dense regions of mass due to a galaxy consisting of mainly compact objects. Due to this "macroscopic approach", the coarse grained density will be bounded from above by the fine grained density:  $F_{\text{cg}} \leq F_{\text{fg}}$ . If we take a closer look at galactic halos, we assume the mass density



of the dark matter in the halo to follow

$$\rho_h(r) = \frac{\rho_0}{\left(\frac{r}{r_c}\right)^{1+\beta} \left(1 + \frac{r}{r_c}\right)^{2-\beta}} \quad (5.3)$$

with  $\rho_0$  the core density,  $r$  the distance from the centre of the galaxy,  $r_c$  the radius of the core of the halo and  $\beta$  a free parameter with  $-1 \leq \beta \leq 0$ . This parameter  $\beta$  is introduced to show what happens to different profiles in these calculations. For example by setting  $\beta$  to 0 we obtain the Navarro-Frenk-White profile (NFW profile). The restriction on  $\beta$  is implemented to ensure the density in the inner part of the galaxy does not increase faster than NFW, which matches observations[17]. In the very outer parts of the dark matter halo ( $r \gg r_c$ ), this density distribution has the same properties as the NFW density profile, regardless of the value of  $\beta$ . Looking at the inner core of the galaxy ( $r \ll r_c$ ), it can be seen that the density equation becomes less complex. Both results are shown below:

$$\rho_h(r) = \begin{cases} \rho_0 \left(\frac{r_c}{r}\right)^{1+\beta} & \text{for } r \ll r_c \\ \rho_0 \left(\frac{r_c}{r}\right)^3 & \text{for } r \gg r_c \end{cases}. \quad (5.4)$$

In order to further investigate the behaviour of neutrinos in bound systems we take a look at the Jeans equations. In this section we will use the previously mentioned  $\beta$  parameter density profile. In appendix A we do the same calculations for the isothermal density profile, which is constant for small  $r$  and falls of  $\propto r^{-2}$  for large  $r$ . The Jeans equations describe the motion of a collection of collisionless objects in a gravitational field. With these equations we will be able to find the one dimensional velocity dispersion of the particles in this gravitational field, which will be used to determine maximum neutrino density in velocity phase space. The Jeans equations are quite complex, but become significantly more manageable when we assume a steady state hydrodynamic equilibrium ( $\partial/\partial t = 0$  and  $\bar{v}_r = 0$ ), where  $\bar{v}_r$  denotes the average radial velocity. Spherical symmetry is also assumed for the dark matter halo, which implies that  $\bar{v}_\theta = 0$ , where  $\bar{v}_\theta$  denotes the tangential velocity. Lastly the velocity dispersion tensor is assumed to be isotropic, which means that  $\sigma_r(r)^2 = \sigma_\theta(r)^2 \equiv \sigma(r)^2$ , the square of the one dimensional velocity dispersion, which is the variance of a Gaussian velocity distribution. This one dimensional velocity dispersion  $\sigma(r)$  is the standard deviation of the velocities. In spherical coordinates the radial Jeans equation is then given by:

$$\frac{\partial(\rho\sigma(r)^2)}{\partial r} + \rho \frac{\partial\Phi}{\partial r} = 0. \quad (5.5)$$

In this equation  $\rho$  denotes the mass density, which in our case is equal to  $\rho_h(r)$ , and  $\Phi$  denotes the gravitational potential. This equation gives us the velocity dispersion if the gravitational potential is known, so we will solve Poisson's equation for gravity to get this potential:

$$\nabla^2\Phi = 4\pi G\rho. \quad (5.6)$$

Writing this in spherical coordinates and substituting the halo mass density  $\rho_h(r)$  as the mass density  $\rho$ , turns this equation into:

$$\frac{1}{r^2} \frac{\partial}{\partial r} \left( r^2 \frac{\partial \Phi}{\partial r} \right) = \frac{4\pi G \rho_0}{\left( \frac{r}{r_c} \right)^{1+\beta} \left( 1 + \frac{r}{r_c} \right)^{2-\beta}}. \quad (5.7)$$

Multiplying by  $r^2$ , integrating both sides from 0 to  $r$  with respect to  $r'$  and introducing  $x \equiv r'/r_c$  for practical purposes:

$$r^2 \frac{\partial \Phi}{\partial r} = 4\pi G \rho_0 r_c^3 \int_0^{\frac{r}{r_c}} x^{1-\beta} (1+x)^{\beta-2} dx. \quad (5.8)$$

This gives the required value for the radial derivative of the gravitational potential:

$$\frac{\partial \Phi}{\partial r} = \frac{4\pi G \rho_0 r_c^3}{r^2} \left[ \frac{x^{2-\beta}}{2-\beta} {}_2F_1(2-\beta, 2-\beta; 3-\beta; -x) \right]_0^{\frac{r}{r_c}}. \quad (5.9)$$

Here  ${}_2F_1(a, b; c; x)$  denotes the hypergeometric function. For small  $x$  the expression  $\frac{x^{2-\beta}}{2-\beta} {}_2F_1(a, b; c; x)$  behaves as  $\frac{x^{2-\beta}}{2-\beta}$ , which means that as  $x \rightarrow 0$  the previous expression also goes to 0. This means equation 5.9 evaluates to

$$\frac{\partial \Phi}{\partial r} = 4\pi G \rho_0 r_c^3 \frac{(r/r_c)^{2-\beta}}{r^2(2-\beta)} {}_2F_1(2-\beta, 2-\beta; 3-\beta; -r/r_c). \quad (5.10)$$

This expression makes it possible to solve the Jeans radial equation. To solve the radial Jeans equation for our dark matter distribution  $\rho_h(r)$ , we need to integrate equation 5.5 with respect to  $r$ :

$$\rho_h(r) \sigma(r)^2 = \rho_0 C - \int_0^r \rho_h(r') \frac{\partial \Phi}{\partial r'} dr'. \quad (5.11)$$

Here  $\rho_0 C$  is a constant due to the boundaries of the integration. In the outer parts of the galaxy, our density profile goes as  $\rho_h(r \gg r_c) \propto r^{-3}$ . Implementing this into the radial Jeans equation shows that the  $r$  dependency of  $\sigma(r)^2$  is less than  $r^3$ . This means that when  $r$  goes to infinity,  $\rho_h(r) \sigma(r)^2$  goes to 0. Implementing this condition into the equation above yields:

$$\lim_{r \rightarrow \infty} \rho_h(r) \sigma(r)^2 = \rho_0 C - \int_0^\infty \rho_h(r') \frac{\partial \Phi}{\partial r'} dr' = 0 \Rightarrow \rho_0 C = \int_0^\infty \rho_h(r') \frac{\partial \Phi}{\partial r'} dr'. \quad (5.12)$$

Substituting this result and the result from equation 5.10 into equation 5.11:

$$\rho_h(r) \sigma(r)^2 = \int_r^\infty \frac{4\pi G \rho_0^2 r_c^3 (r'/r_c)^{2-\beta}}{\left( \frac{r'}{r_c} \right)^{1+\beta} \left( 1 + \frac{r'}{r_c} \right)^{2-\beta}} \frac{{}_2F_1(2-\beta, 2-\beta; 3-\beta; -r'/r_c)}{(r')^2(2-\beta)} dr'. \quad (5.13)$$

Again substituting  $x \equiv r'/r_c$  yields

$$\rho_h(r) \sigma(r)^2 = \frac{4\pi G \rho_0^2 r_c^2}{2-\beta} \int_{r/r_c}^\infty \frac{{}_2F_1(2-\beta, 2-\beta; 3-\beta; -x)}{(1+x)^{2-\beta} x^{1+2\beta}} dx. \quad (5.14)$$

This gives us an expression for  $\sigma(r)^2$  which can be used to calculate the maximum velocity phase space density. Velocity distributions in dark matter halos are usually modelled by a Maxwellian velocity distribution [18]. This models a large number of non relativistic, non interacting particles. This model is backed up by the fact that equation 5.2 turns into a Maxwellian distribution when  $m_\nu v^2 \gg 2K_B T$ . The fraction of particles in an infinitesimal volume of velocity phase space  $d^3v$  is equal to

$$f(v)d^3v = \frac{1}{(2\pi\sigma(r)^2)^{\frac{3}{2}}} e^{-\frac{v^2}{2\sigma(r)^2}} d^3v. \quad (5.15)$$

The maximum value of this function is equal to  $(2\pi\sigma(r)^2)^{-\frac{3}{2}}$ . This will be used when we are looking for the maximum coarse grained six-dimensional phase space mass density. The coarse grained six-dimensional phase space mass density is equal to the product of the velocity phase space number density and the position space mass density. These values can be found in equations 5.15 and 5.3. Combining these two yields a coarse grained six-dimensional phase space mass density of

$$F_{\text{cg}}(r) = \frac{\rho_h(r)}{(2\pi\sigma(r)^2)^{\frac{3}{2}}}. \quad (5.16)$$

The maximum value for the coarse grained six-dimensional phase space mass density can now be calculated for any value of  $\beta$  if the core radius and core density for this model are known. One of the most popular models is the Navarro–Frenk–White density profile. Our  $\beta$  dependent density profile becomes the NFW profile when  $\beta$  is set to 0. The values for the core density and core radius in this model are known to be  $r_c = 24.42$  kpc and  $\rho_0 = 0.184$  (GeV/ $c^2$ )/cm<sup>3</sup>. When  $\beta$  is set to 0, equation 5.14 shows  $\sigma(r)^2$  to be equal to:

$$\sigma(r)^2 = 2\pi G \rho_0 r_c^2 \left(\frac{r}{r_c}\right) \left(1 + \frac{r}{r_c}\right)^2 \int_{r/r_c}^{\infty} \frac{{}_2F_1(2, 2; 3; -x)}{(1+x)^2 x} dx. \quad (5.17)$$

Substituting this result into equation 5.16 shows that  $F_{\text{cg}}(r)$  has no maximum, as it diverges to infinity as  $r$  goes to 0. Our calculations however, depend on the assumption of a continuous density profile. This assumption is not justified for the very inner parts of the galaxy, because these parts of the galaxy are more granular. Black holes for example will trap a lot of matter into a small part of space, which resembles a more discrete mass distribution. The transition between a more continuous to a more discrete looking distribution of mass is not exactly defined, but for profiles that are similar to our  $\beta$  dependent density profile innermost resolved radii  $\sim 10^{-2} r_{\text{vir}} \approx 2$  kpc are used, and we will denote this minimum value for the radius as  $r_*$  [19]. Since this is a bit of a flexible cutoff, we will also look at a radius of 3 kpc to see the impact of moving this cutoff point. The NFW profile has a known core density and radius, being  $r_c = 24.42$  kpc and  $\rho_0 = 0.184$  (GeV/ $c^2$ )/cm<sup>3</sup>[20]. Substituting these values into the above equations yields the maximum six-dimensional coarse grained

phase space mass density:

$$F_{\text{cg,NFW}}(r_*) = \frac{\left(\frac{r_*}{r_c}\right)^{-\frac{5}{2}} \left(1 + \frac{r_*}{r_c}\right)^{-5}}{(2\pi)^3 \rho_0^{\frac{1}{2}} r_c^3 \left(G \int_{r_*/r_c}^{\infty} \frac{{}_2F_1(2,2;3;-x)}{(1+x)^2 x} dx\right)^{\frac{3}{2}}} \quad (5.18)$$

We know that the maximum coarse-grained six dimensional phase space mass density is bounded from above by its fine-grained counterpart from equation 5.2, which leads to a bound on the neutrino mass:

$$F_{\text{cg,NFW}}(r_*) \leq \frac{g_\nu m_\nu^4}{2h^3}. \quad (5.19)$$

$$m_\nu \geq \left(\frac{2h^3 F_{\text{cg,NFW}}(r_*)}{g_\nu}\right)^{\frac{1}{4}}. \quad (5.20)$$

This leaves us with a constraint on the allowed mass of the neutrino mass eigenstates bound to the centre parts of a dark matter halo. Taking  $g_\nu = 4$  for the number of combinations of two spin states and particle or antiparticle for one neutrino species, we obtain

$$m_\nu \geq \left(\frac{2h^3 F_{\text{cg,NFW}}(r_*)}{g_\nu}\right)^{\frac{1}{4}} = 44.89 \frac{\text{eV}}{c^2}. \quad (5.21)$$

The same process for an innermost resolved radius of  $r_* = 3$  kpc gives a value of  $m_\nu \geq 37.27 \text{ eV}/c^2$ . This equation only takes into account one type of neutrino, but the sum of the neutrino masses is orders of magnitude smaller than this number [21], so dark matter has to be predominantly explained by some other (exotic) form of dark matter. It is important to note here that we solved the Jeans equations for a mass density profile which only accounted for dark matter. This means that a part of this mass can be supplied by the non-dark matter. Since our result shows that the required neutrino mass is multiple orders of magnitude larger than the masses the CDDE model can produce, it is safe to say that even when all the assumptions are accounted for, bound neutrinos cannot explain all dark matter. This leads us to a follow-up question; we have only investigated neutrinos that are bound to galaxies, but the CDDE model can also produce neutrinos that are not bound to galaxies. These neutrinos will function as a "background", and its effects on the cosmic neutrino background (CNB) will be investigated in sections 6 and 7.

## 6 CNB temperature

### 6.1 Introduction to the CNB

As discussed at the end of section 4, it is possible for the neutrinos created in the CDDE model to impact the so called cosmic neutrino background (CNB). As such it is instructive to look at what the CNB is, and to look at its properties. The CNB is a relic of the Big Bang, where all electrons, protons, neutrons and neutrinos were in thermal equilibrium, due to weak force interactions. When the universe cooled to approximately 1 MeV at  $z = 3 \cdot 10^9$  [14], neutrinos decoupled from the other matter [22]. Neutrino decoupling means that the neutrinos do not have a significant amount of interaction anymore with the other matter present. Neutrinos only very rarely interact with matter, and as such there is a background of neutrinos all over the universe, which is called the CNB. One important property of the CNB is its current temperature, and this will be derived in subsection 6.3. This temperature can be used to take a look at the current CNB neutrino number density in the universe. Comparing this number density to the number density of the CDDE neutrinos gives insight into the possibility of "noise" in the CNB due to CDDE neutrinos.

### 6.2 CNB pressure and energy density

In order to derive the CNB temperature and number density in subsection 6.3, some intermediate results are necessary. In this section the energy density and pressure of the CNB will be derived along with the photon energy density in order to calculate the so called effective number of degrees of freedom  $g_f$ . I however find "effective energy density contribution parameter" a better descriptor for what this parameter entails, and as such this will be what  $g_f$  will be called in this bachelor thesis.

To calculate the energy densities it is assumed that the universe is isotropic, which is supported by the measurements that show large scale isotropy in the current universe [5]. A thermal equilibrium is also assumed, because the collision rate between photons and charged particles was significantly larger than the expansion rate of the early universe. Thermal equilibrium in an isotropic universe implies that the matter in the universe expands adiabatically. The entropy per comoving volume stays constant over an adiabatic reversible process[23], and as the universe expands, this comoving volume will scale with  $a^3$  so:

$$s(T)a^3 = \text{constant}, \quad (6.1)$$

with  $s(T)$  the entropy density of the universe which depends on the temperature. The second law of thermodynamics then tells us that the change in entropy in

a system of volume  $V$  due to an adiabatic change is given by:

$$d(s(T)V) = \frac{d(\rho(T)V) + p(T)dV}{T} \quad (6.2)$$

Expanding the brackets leads to

$$ds(T)V + dVs(T) = \frac{d\rho(T)V + \rho(T)dV + p(T)dV}{T}, \quad (6.3)$$

and looking at the terms with  $dV$  gives us the entropy density:

$$s(T) = \frac{\rho(T) + p(T)}{T} \quad (6.4)$$

Equating the  $dT$  terms and using equation 6.4 gives us conservation of energy:

$$T \frac{dp(T)}{dT} = \rho(T) + p(T) \quad (6.5)$$

In order to find the energy density of the CNB and the photons we start out with the number density of a species of particle/antiparticle with  $|\vec{p}|$  between  $p$  and  $p + dp$ , which is given by:

$$n(p, T)dp = \frac{4\pi g_s p^2 dp}{(2\pi\hbar)^3} \left( \frac{1}{e^{\sqrt{p^2 + m^2}/K_B T} \pm 1} \right) \quad (6.6)$$

This result is obtained by taking the number of momentum states per volume element with  $|\vec{p}|$  between  $p$  and  $p + dp$  and multiplying this by the average distribution (Fermi-Dirac or Bose-Einstein) for this momentum state. This equation uses a  $+$  for fermions and a  $-$  for bosons. Here  $K_B$  denotes the Boltzmann constant and the  $g_s$  in this equation is equal to the amount of independent spin states of the particle, which for spin 1/2 fermions is 2. For photons this is also 2 due to the two possible helicity values. It is now possible to express the energy density as follows:

$$\rho(T) = \int_0^\infty n(p, T) dp \sqrt{p^2 + m^2} \quad (6.7)$$

Here the energy density equation is simply given by integrating the number density multiplied by the corresponding energy over the entire momentum space.

The derivation for the pressure is a little more complex. Assume space to be homogeneously and isotropically filled with particles and let's look at a small area  $dA$ , with a normal vector to this area called  $\hat{n}$ . We then know that all the particles that hit this area with a velocity of  $\vec{v} = |\vec{v}|\hat{v} \equiv v\hat{v}$  between  $t$  and  $t + dt$  must be located on a spherical shell with radius  $R = vt$  and a thickness of  $vdt$ . A graphical representation of this is given in figure 4 below: We can then

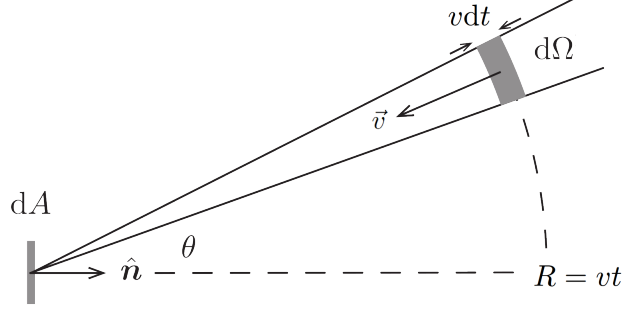


Figure 4: A graphical representation of the volume element  $dV$ . Modified from [24]

express the corresponding volume element  $dV$  on this shell by using the solid angle spanned by this volume element  $d\Omega \equiv \sin\theta d\theta d\phi$ :

$$dV = R^2 v d\Omega dt \quad (6.8)$$

Multiplying this by the number density 6.6 we obtain the number of particles in this volume element  $dNdp$  with  $|\vec{p}|$  between  $p$  and  $p + dp$ ;

$$dNdp = n(p, T) dp R^2 v d\Omega dt \quad (6.9)$$

We need to take into account that only the particles directed at the surface area will reach the area, so with the previous condition of isotropy we can find the total number of relevant particles reaching the area element  $dA$  with velocity direction  $\hat{v}$  to be:

$$dN_A dp = \frac{|\hat{v} \cdot \hat{n}|}{8\pi R^2} dA dNdp = \frac{|\hat{v} \cdot \hat{n}|}{8\pi} n(p, T) v dp d\Omega dt dA, \quad (6.10)$$

where we have an extra factor  $\frac{1}{2}$  due to only the negative values of  $\hat{v} \cdot \hat{n}$  contributing. We know that pressure can be seen as the change of momentum per unit of area per unit of time, and we know that a particle that bounces elastically off a wall with normal vector  $\hat{n}$  transfers  $2|\vec{p} \cdot \hat{n}|$  of its momentum. This means the total pressure contribution of the particles with  $|\vec{p}|$  between  $p$  and  $p + dp$  will be given by:

$$\rho_P(p, T) dp = 2p dp \int \frac{|\hat{v} \cdot \hat{n}|}{dA dt} dN_A = \frac{n(p, T)}{4\pi} p v dp \int (\hat{v} \cdot \hat{n})^2 d\Omega, \quad (6.11)$$

where we have used that the direction of  $\vec{p}$  and  $\vec{v}$  are the same, so  $|\vec{p} \cdot \hat{n}| = p|\hat{v} \cdot \hat{n}|$ . If we then use that  $v = p/E$  we obtain:

$$\rho_P(p, T)dp = n(p, T) \frac{p^2 dp}{4\pi E} \int_0^{2\pi} d\phi \int_0^\pi \cos^2(\theta) \sin(\theta) d\theta, \quad (6.12)$$

where we have used that the area element  $d\Omega = \sin(\theta)d\theta d\phi$  and that  $|\hat{v} \cdot \hat{n}|^2 \equiv \cos^2(\theta)$ . Integrating over  $dp$  gives the equation for the total amount of pressure:

$$P(T) = \int_0^\infty n(p, T) dp \frac{p^2}{3\sqrt{p^2 + m^2}} \quad (6.13)$$

In the early universe all matter is ultra relativistic, so we take a look at the ultra relativistic limit:  $p \gg m$ . In this limit equations 6.7 and 6.13 show that  $P(T) = \rho(T)/3$  which in turn makes equation 6.5 turn into the Stefan-Boltzmann law ( $\rho = g_f a_B T^4$ ) where  $g_f$  denotes the effective energy density contribution parameter and  $a_B$  is a constant. These coefficients follow from the equation below:

$$\rho(T) = g_s \int_0^\infty \frac{4\pi p^3 dp}{(2\pi\hbar)^3} \left( \frac{1}{e^{p/K_B T} \pm 1} \right). \quad (6.14)$$

Here the minus sign is for bosons, and the plus sign for fermions. When we substitute  $x = \frac{p}{K_B T}$ , this simplifies to:

$$\rho(T) = \frac{g_s}{2\pi^2 \hbar^3} \int_0^\infty \frac{p^3 dp}{e^{p/K_B T} \pm 1} = \frac{g_s T^4 K_B^4}{2\pi^2 \hbar^3} \int_0^\infty \frac{x^3 dx}{e^x \pm 1}. \quad (6.15)$$

The integral part evaluates to:

$$\int_0^\infty \frac{x^3 dx}{e^x \pm 1} = \begin{cases} 6Li_4(1) = \frac{\pi^4}{15} & \text{for bosons}(-) \\ -6Li_4(-1) = \frac{7\pi^4}{120} & \text{for fermions}(+) \end{cases}, \quad (6.16)$$

where Li represents the polylogarithm. This means that  $\rho(T)$  evaluates to:

$$\rho(T) = \begin{cases} \frac{g_s K_B^4 \pi^2}{30\hbar^3} T^4 = \frac{K_B^4 \pi^2}{15\hbar^3} T^4 & \text{for photons} \\ \frac{7g_s K_B^4 \pi^2}{240\hbar^3} T^4 = \frac{7K_B^4 \pi^2}{120\hbar^3} T^4 & \text{for spin } \frac{1}{2} \text{ fermions} \end{cases}, \quad (6.17)$$

where  $g_s$  is 2 for spin- $\frac{1}{2}$  fermions due to the two spin states and also 2 for photons due to the helicity. If we now introduce a constant  $a_B = \frac{K_B^4 \pi^2}{30\hbar^3}$  then equation 6.17 reduces to:

$$\rho(T) = \begin{cases} 2a_B T^4 & \text{for photons} \\ \frac{7}{4}a_B T^4 & \text{for spin } \frac{1}{2} \text{ fermions} \end{cases}. \quad (6.18)$$



### 6.3 CNB temperature and number density

The universe was at thermal equilibrium before neutrinos decoupled, and since both the photon temperature and the neutrino temperature cooled by cosmic expansion, both temperatures stayed equal. This is until the temperature dropped below the temperature needed for two photons to create an electron-positron pair ( $\gamma\gamma \rightarrow e^+e^-$ ), and only electron-positron annihilation ( $e^+e^- \rightarrow \gamma\gamma$ ) remained. The positrons and electrons transferred their heat and entropy to the photons which in turn increased the photon temperature. This means the ratio of the temperature of the photons before the electron-positron annihilation and the temperature after is the same as the ratio of the temperature of the neutrinos and the temperature of the photons after annihilation. We assume the entropy to be approximately conserved, giving us:

$$s \propto g_f T^3 \quad (6.19)$$

This equation is obtained by recalling that in the ultra relativistic limit  $P(T) = \rho(T)/3$ , and using this result with equation 6.4. Once all the reactions stop, the entropy will vary very little for temperatures below the temperature where most positrons and electrons annihilated and we can use equation 6.19 to find:

$$\frac{T_1}{T_2} = \left( \frac{g_2}{g_1} \right)^{\frac{1}{3}} \quad (6.20)$$

The neutrino temperature  $T_1 \propto T_\nu$  is the lowest temperature where the production and annihilation of electron-positron pairs are still in equilibrium and the photon temperature  $T_2 \propto T_\gamma$  is a slightly higher temperature, because of the transferred heat from the positron-electron annihilation. The coefficients  $g_1$  and  $g_2$  are determined by a sum, based on the effective energy density contribution parameters of the associated particles. These can be seen in equation 6.17.  $T_1$  has electron-positron creation and annihilation influencing the photon temperature, so it sums the influence of these three particles.  $T_2$  only has photons, so  $g_2$  is simply 2, and this gives us the ratio between the temperatures:

$$\frac{T_\nu}{T_\gamma} = \frac{T_1}{T_2} = \left( \frac{g_2}{g_1} \right)^{\frac{1}{3}} = \left( \frac{2}{2 + \frac{7}{4} + \frac{7}{4}} \right)^{\frac{1}{3}} = \left( \frac{4}{11} \right)^{\frac{1}{3}} \approx 0.714 \quad (6.21)$$

With a present-day CMB temperature of  $T_{\gamma,0} = 2.725\text{K}$  [25] we can then calculate the present-day CNB temperature:

$$T_{\nu,0} = \left( \frac{4}{11} \right)^{\frac{1}{3}} T_{\gamma,0} \approx 1.95\text{K} \quad (6.22)$$

Note that the result of the equation above assumes the neutrinos to be ultra-relativistic, and as such will almost certainly not be applicable to the highest mass eigenstate. The CNB temperature is needed to calculate the current CNB number density, which will be used to look at the effect of the neutrinos created

in the CDDE model on the CNB. Integrating the number density of a neutrino with its momentum  $|\vec{p}|$  between  $p$  and  $p + dp$  from equation 6.6, gives the (anti)neutrino mass eigenstate number density as a function of temperature in the relativistic limit:

$$\rho_N(T) = \int_0^\infty \frac{4\pi p^2 dp}{(2\pi\hbar)^3} \left( \frac{1}{e^{p/K_B T} + 1} \right) \quad (6.23)$$

$$= \frac{1}{\pi^2 \hbar^3} \int_0^\infty \frac{p^2 dp}{e^{p/K_B T} + 1} = \frac{T^3 K_B^3}{\pi^2 \hbar^3} \int_0^\infty \frac{x^2 dx}{e^x + 1} = \frac{T^3 K_B^3}{\pi^2 \hbar^3} \frac{3\zeta(3)}{2}. \quad (6.24)$$

It is now possible to find the current CNB (anti)neutrino mass eigenstate number density, by substituting the current CNB temperature value and multiplying by  $c^3$ , to compensate for natural units;

$$\rho_N(T_{\nu,0}) \approx 5.62 \cdot 10^7 \text{m}^{-3}. \quad (6.25)$$

This is the number density for one single mass eigenstate of neutrino, or one mass eigenstate of antineutrino. This calculation rests on the assumption of enough energy in the early universe, to not have a preference for mass eigenstates, and equal amounts of matter and antimatter being produced. This result cannot be used for the highest mass eigenstate, due to the assumption of relativistic particles. A follow-up study will need to look at the epoch when certain neutrinos become non relativistic. The influence of this assumption on our results will be discussed in section 7.2.

## 7 Filling the universe and CNB noise

To obtain the correct numerical results, this section will *not* use  $c = \hbar = 1$ .

### 7.1 Filling the universe

Neutrinos cannot all be bound, so can neutrinos be the particles that describe our matter creation. To look into this question we take a look at the fermi energy of ground state neutrinos in a box, which is equal to:

$$E_F = \frac{\hbar^2}{2m_\nu} \left( \frac{6\pi^2}{2S+1} \right)^{\frac{2}{3}} \rho_N^{\frac{2}{3}} = \frac{\hbar^2}{2m_\nu} (3\pi^2)^{\frac{2}{3}} \rho_N^{\frac{2}{3}}. \quad (7.1)$$

Here  $S$  denotes the spin value of the particles, which for neutrinos is equal to  $\frac{1}{2}$ . Rewriting this as a function of  $\rho_N$  gives:

$$\rho_N = \left( \frac{2m_\nu E_F}{\hbar^2} \right)^{\frac{3}{2}} \frac{1}{3\pi^2}. \quad (7.2)$$

We recall that the CDDE model only has the possibility to create non-relativistic particles, so the Fermi energy, which is equal to the kinetic energy of the highest energy particle is given by  $E_{kin} = \frac{1}{2}m_\nu v_F^2 = E_F$ . Substituting this in the previous equation gives us the particle density as a function of the velocity of the neutrino with the highest velocity

$$\rho_N = \frac{1}{3\pi^2} \left( \frac{m_\nu v_F}{\hbar} \right)^3. \quad (7.3)$$

The total contribution to the mass of the observable universe is given by the number density multiplied by the volume of the universe  $V_U$  and the mass of the neutrino  $m_\nu$ :

$$m_{tot,\nu} = \rho_N V_U m_\nu = \frac{V_U m_\nu}{3\pi^2} \left( \frac{m_\nu v_F}{\hbar} \right)^3. \quad (7.4)$$

The created dark matter particles in the CDDE model add 57% extra mass on top of the mass in the  $\Lambda$ -CDM model. Using this information it is possible to calculate the relation between the neutrino mass and the Fermi velocity which makes this amount of mass possible:

$$m_{tot,\nu} = 0.57 m_{tot,U} \Rightarrow m_\nu^4 v_F^3 = \frac{1.71 \pi^2 \hbar^3 m_{tot,U}}{V_U}. \quad (7.5)$$

Using this ratio it is possible to determine the needed mass of neutrinos in order to achieve this amount of extra mass. We recall that we cannot produce relativistic neutrinos, and since the threshold for relativistic particles is a little ambiguous, we will take relativistic particles to be particles whose kinetic energy is in the same order of magnitude as the mass. The kinetic energy of a relativistic particle with mass  $m_0$  is given by:

$$E_{kin} = (\gamma - 1)m_0 c^2. \quad (7.6)$$

Here  $\gamma \equiv 1/\sqrt{1-v^2/c^2}$ . Equating this to the mass energy of a particle at rest:

$$m_0 c^2 = (\gamma - 1)m_0 c^2 \Rightarrow \gamma = 2 \Rightarrow v = \frac{\sqrt{3}}{2}c \approx 0.866c. \quad (7.7)$$

We substitute this result into the Fermi velocity of equation 7.5 to obtain the minimal value for the lowest neutrino mass eigenstate which allows this neutrino to account for the 57% mass increase

$$m_\nu \geq \left( \frac{8 \cdot 1.71 \pi^2 \hbar^3 m_{tot,U}}{3\sqrt{3} V_U c^3} \right)^{\frac{1}{4}} \approx 3.99 \frac{\text{meV}}{c^2}. \quad (7.8)$$

Here the value for  $m_{tot,U}$  has been taken to be approximately  $\frac{1}{0.15} \cdot 1.2 \cdot 10^{53} = 8 \cdot 10^{53} \text{kg}$ . Where  $1.2 \cdot 10^{53} \text{kg}$  is the total "non-dark" mass of the universe[26], and the fraction  $\frac{1}{0.15}$  comes from 85% of the total mass being dark matter and 15% "non-dark" matter[27]. The value for  $V_U$  is equal to  $3.57 \cdot 10^{80} \text{m}^3$  [28]. With this minimal neutrino mass eigenstate mass, it can now be said that in the CDDE model, the 57% extra mass can be accommodated by neutrino production, if two conditions are met.

- 1: *The mass of the lowest neutrino mass eigenstate must be larger than the bound in equation 7.8.*
- 2: *The neutrino mass must be in the meV range to be eligible for production in the CDDE model.*

The order of mass eigenstates is currently unknown, but has been reduced to two options: normal hierarchy and inverted hierarchy as can be seen in figure 2. If the so called "normal hierarchy" is correct, then the difference between the two lightest mass eigenstates is around 8 meV [8]. This means that if the lightest mass eigenstate is below the above-given bound, the second lightest mass eigenstate will be eligible for production in the CDDE model, and can thus account for the 57% mass increase. If the "inverted hierarchy" is correct, then the difference between the lowest two eigenstates is around 50 meV. This means that if the lowest mass eigenstate neutrino is lighter than the above-given minimum, neutrinos cannot account for the 57% mass increase, due to the fact that, if at all possible, the production of the second lightest mass eigenstate by the CDDE model will be heavily suppressed. This means some other particle will have to provide an additional contribution to the extra 57% of mass in the universe, or the mass creation in the CDDE model has ended prematurely. An explicit model for mass creation is needed to research the second possibility, which is outside the scope of a bachelor thesis.

## 7.2 CNB noise

The creation of the highest neutrino mass eigenstate is, if at all possible, heavily suppressed in the CDDE model. This means that the noise produced by CDDE neutrinos when measuring the CNB will be negligible for heavy mass

eigenstates. This means we will only look at the lighter mass eigenstates, which justifies the assumption of ultrarelativistic CNB neutrinos when calculating the CNB number density. In order to take a look at this possible noise in CNB measurements due to CDDE neutrinos, the neutrino number density needs to be calculated. This is done by combining equations 7.4 and 7.5 to yield:

$$\rho_N = \frac{0.57 m_{tot,U}}{m_\nu V_U} \quad (7.9)$$

The question now arises of what mass to choose for this equation. The CDDE model only allows for creation in the meV range, so we will choose a mass of 10 meV to probe the density. This gives us an expression for the neutrino number density:

$$\rho_N = \frac{0.57 \cdot 4.49 \cdot 10^{89} \text{eV}}{3.57 \cdot 10^{80} \text{m}^3 \cdot 10 \text{ meV}} \approx 7.17 \cdot 10^{10} \text{m}^{-3}. \quad (7.10)$$

This is the number density for all neutrino mass eigenstates and all antineutrino mass eigenstates combined. This shows there will be a significantly higher amount of neutrinos present in a CDDE universe than expected from just the CNB. Trying to detect neutrinos is notoriously difficult, and experiments like PTOLEMY detect neutrinos by using an interaction involving an electron neutrino. This type of experiment only measures neutrinos that are in the electron flavour eigenstate, and since certain mass eigenstates favour certain flavour eigenstates, experiments using such a detection method will have a bias towards certain mass eigenstates. This means that until experiments have a sufficiently high resolution to be able to distinguish the mass eigenstates of the electron neutrino, it is important to take the differing flavour components of the mass eigenstates into account when predicting noise. The order of the hierarchy of masses is currently unknown, but it has been narrowed down to two options called "normal hierarchy" and "inverted hierarchy". In the following two subsections we will take a look the impact of CDDE neutrinos at experiments that only detect *electron neutrinos*, such as PTOLEMY.

### 7.2.1 Inverted hierarchy

In the inverted hierarchy, the gap between the lowest two neutrino mass eigenstates is approximately 50 meV. This means the production of  $\nu_2$  is either not possible or heavily suppressed, so we only have to take a look at  $\nu_1$ . Since  $\nu_1$  has in that case an electron flavour component of  $\approx 2.5\%$  [8], 2.5% of the produced CDDE neutrinos will be in the electron flavour eigenstate. Let's assume the CNB neutrino mix to consist of equal parts electron, muon and tau neutrinos. This is justified because the early universe was energetic enough to produce all three mass eigenstates and neutrino oscillation will then cause an approximately equal flavour split for CNB neutrinos. Let's also assume CNB and CDDE neutrinos to be made up of an equal amount of neutrinos and antineutrinos. Combining these assumptions and the results from equations 6.25 and 7.10, we can calculate the amount of electron (anti)neutrinos from the CDDE

model per electron (anti)neutrino from the CNB. The total number density of CDDE electron (anti)neutrinos will be equal to

$$0.025 \cdot 0.5 \cdot 7.17 \cdot 10^{10} \text{m}^{-3} = 8.96 \cdot 10^8 \text{m}^{-3} \quad (7.11)$$

because 2.5% of  $\nu_1$  are in the electron flavour eigenstate, and half the neutrinos are assumed to be antineutrinos. This factor of 0.5 should be removed in the case that neutrinos are majorana particles. A similar approach for CNB electron neutrinos with indistinguishable mass eigenstates, would be done by multiplying the CNB density from equation 6.25 by 3, for the three mass eigenstates, and subsequently dividing by 3, because one third of those neutrinos is in the electron flavour eigenstate. There is no factor 0.5 for antineutrinos here, since equation 6.25 already gives the density for neutrinos or antineutrinos. This calculation trivially returns the value of  $5.62 \cdot 10^7 \text{m}^{-3}$ , which would mean there would be approximately 15.9 CDDE neutrinos measured for every CNB neutrino. If it is the case that the experiment can distinguish between the mass eigenstates of the measured *electron* neutrinos, then the CNB electron flavour density of  $\nu_1$  would be given by:

$$0.025 \cdot 5.62 \cdot 10^7 \text{m}^{-3} \approx 1.41 \cdot 10^6 \text{m}^{-3}. \quad (7.12)$$

This means that an experiment that can distinguish between mass eigenstates will detect approximately 635 CDDE  $\nu_1$  electron neutrinos for every CNB neutrino in the same state. This noise means that the CNB cannot properly be observed by measuring the lowest mass eigenstate component of the electron neutrinos. An important assumption here is that this result is dependent on the lowest mass eigenstate being equal to 10 meV. If the energy of the lowest mass eigenstate was equal to 1 meV, there would be 10 times more CDDE neutrinos, as can be seen from equation 7.9, and the ratio would become 1 CNB neutrino to 159 CDDE neutrinos for experiments that cannot distinguish mass eigenstates, and 1 to 6350 for experiments that can. A lowest mass eigenstate of 30 meV would yield 3 times less noise on CNB measurements, but the production of neutrinos around this mass would get increasingly suppressed. This implies that if the universe gains 57% extra mass, due to CDDE model neutrino production, electron based CNB detection experiments will measure significantly more CDDE neutrinos than CNB neutrinos. If the mass is lower than 10 meV, the share of CNB neutrinos will become substantially smaller.

### 7.2.2 Normal hierarchy

If normal hierarchy is the correct hierarchy, there will be a mass gap of approximately  $8 \text{ meV}/c^2$  from  $\nu_1$  to  $\nu_2$ .  $\nu_1$  and  $\nu_2$  will have an electron neutrino component of approximately  $2/3$  and  $1/3$  respectively [8]. The CDDE model has a possibility of producing two neutrino mass eigenstates, and information about the working of neutrino production in the CDDE model, and values for the mass eigenstates are needed to calculate the ratio of produced  $\nu_1$  to  $\nu_2$ . This means we will make the assumption that the production of  $\nu_2$  is suppressed,

since the production of higher masses gets suppressed by the CDDE model. If all the neutrinos are in the lowest mass eigenstate, that leads to a number density of

$$\rho_N = \frac{2}{3} \cdot 0.5 \cdot 7.17 \cdot 10^{10} \text{m}^{-3} \approx 2.39 \cdot 10^{10} \text{m}^{-3} \quad (7.13)$$

$\nu_1$  in the electron flavour state. This will result in approximately 425 times more CDDE electron neutrinos than CNB for experiments that do not distinguish mass eigenstates, and 635 times more CDDE neutrinos for experiments that do distinguish between mass eigenstates. It is important to note that these calculations depend on all the neutrinos being in the lowest mass eigenstate. In this hierarchy it is very plausible that the second mass eigenstate is eligible for creation by the CDDE model. But the production of this mass eigenstate will be suppressed because it is heavier, and even if the model produces significantly less  $\nu_1$ , because of  $\nu_2$  production, the CDDE neutrinos will still significantly outnumber the CNB neutrinos.

## 8 Outlook and conclusions

In this thesis we showed a process for determining the minimum mass that a fermionic particle must have to obey the Jeans equations for a gravitationally self sustained density profile. Calculations were done for two different density profiles (NFW and isothermal) with similar results. These calculations showed that neutrinos produced by the CDDE model cannot explain all dark matter, and thus a different form of (exotic) dark matter still has to account for the effects seen in galaxies. This lead to the investigation of neutrinos that are not bound to galaxies. It was shown that all the extra matter created in the CDDE model can be explained by neutrinos, if a produced neutrino mass eigenstate is heavier than  $3.99 \frac{\text{meV}}{c^2}$ . This means that if the neutrino mass eigenstates are ordered as the normal hierarchy, then the 57% mass increase will be accomodated by neutrinos if  $\nu_1$  is light enough to be produced by the CDDE model. It was shown that in the inverted hierarchy,  $\nu_1$  has to be light enough to be produced *and* heavier than  $2.24 \frac{\text{meV}}{c^2}$  to account for the 57% mass increase. The number densities of the CNB and the neutrinos produced by the CDDE model were calculated, and the electron components of the respective models were compared. It was shown that for a lowest mass eigenstate of  $10 \frac{\text{meV}}{c^2}$ , the lowest ratio between CDDE and CNB neutrinos, is equal to 15.9 CDDE neutrinos for every CNB neutrino. This is the case when neutrino masses are ordered by inverted hierarchy, and the experiment cannot distinguish between mass eigenstates of the electron neutrinos. This shows that even if the lowest neutrino mass is heavier than  $10 \frac{\text{meV}}{c^2}$ , CDDE neutrinos will outnumber CNB neutrinos significantly if the CDDE neutrinos can account for the 57% mass increase in the universe. This would make detecting the influence from CNB neutrinos in electron based detection very hard, if possible at all for light  $\nu_1$ .

Possible future research could look deeper into the workings of the CDDE model, to discover what the limits on particle production are. These limits would make it possible to make more precise statements about the amount of noise in the CNB due to CDDE neutrinos, without knowing the neutrino mass.

Lastly I would like to mention the upcoming research by Pieter Oosterhoff. He will be doing additional research about the effects of neutrino production in the CDDE model on the measurements of the upcoming PTOLEMY experiment and the non-relativistic aspects of late-time neutrinos.



## A Jeans equations for an isothermal density profile.

The isothermal mass profile is given by:

$$\rho_{\text{iso}}(r) = \frac{\rho_0}{1 + \left(\frac{r}{r_c}\right)^2}. \quad (\text{A.1})$$

The poisson equation is again:

$$\nabla^2 \Phi = 4\pi G \rho. \quad (\text{A.2})$$

Writing this in spherical coordinates, substituting the isothermal mass density  $\rho_{\text{iso}}(r)$  as the mass density  $\rho$  and recalling that  $\rho_{\text{iso}}(r)$  is spherically symmetric turns this equation into:

$$\frac{1}{r^2} \frac{\partial}{\partial r} \left( r^2 \frac{\partial \Phi}{\partial r} \right) = 4\pi G \frac{\rho_0}{1 + \left(\frac{r}{r_c}\right)^2}. \quad (\text{A.3})$$

Multiplying by  $r^2$ , and integrating both sides with respect to  $r'$  from 0 to  $r$ :

$$r^2 \frac{\partial \Phi}{\partial r} = \int_0^r 4\pi G \rho_0 \frac{r'^2}{1 + \left(\frac{r'}{r_c}\right)^2} dr' = 4\pi G \rho_0 r_c^2 \left( r - r_c \arctan \left( \frac{r}{r_c} \right) \right). \quad (\text{A.4})$$

Dividing both sides by  $r^2$  yields the spatial derivative of the gravitational potential in our density profile

$$\frac{\partial \Phi}{\partial r} = 4\pi G \rho_0 \left( \frac{r_c}{r} \right)^2 \left( r - r_c \arctan \left( \frac{r}{r_c} \right) \right). \quad (\text{A.5})$$

It is now possible to solve the spherical Jeans equation as described in equation 5.5, by substituting the expression found above for  $\frac{\partial \Phi}{\partial r}$ , and the isothermal density profile  $\rho_{\text{iso}}(r)$  as the density:

$$\frac{\partial}{\partial r} \rho_{\text{iso}}(r) \sigma(r)^2 = -4\pi G \rho_0^2 \left( \frac{r_c}{r} \right)^2 \frac{(r - r_c \arctan \left( \frac{r}{r_c} \right))}{1 + \left(\frac{r}{r_c}\right)^2}. \quad (\text{A.6})$$

This equation can be solved by integrating both sides from 0 to  $r$ :

$$\rho_{\text{iso}}(r) \sigma(r)^2 = \rho_0 C - 4\pi G \rho_0^2 r_c \int_0^r \left( \frac{r_c}{r'} \right)^2 \frac{\frac{r'}{r_c} - \arctan \left( \frac{r'}{r_c} \right)}{1 + \left(\frac{r'}{r_c}\right)^2} dr'. \quad (\text{A.7})$$

Introducing the substitution  $x = r'/r_c$  to solve the integral gives:

$$\rho_{\text{iso}}(r) \sigma(r)^2 = \rho_0 C - 4\pi G \rho_0^2 r_c^2 \int_0^{r/r_c} \frac{dx}{x^2(1+x^2)} (x - \arctan(x)). \quad (\text{A.8})$$

Here  $C$  is a constant due to integration. To find a value for  $\rho_0 C$  we again implement the constraint that  $\rho_{\text{iso}}(r)\sigma(r)^2$  must go to 0 when  $r$  goes to infinity. This gives us

$$\lim_{r \rightarrow \infty} \rho_{\text{iso}}(r)\sigma(r)^2 = \rho_0 C - 4\pi G \rho_0^2 r_c^2 \int_0^\infty \frac{dx}{x^2(1+x^2)}(x - \arctan(x)) = 0, \quad (\text{A.9})$$

$$\rho_0 C = 4\pi G \rho_0^2 r_c^2 \int_0^\infty \frac{dx}{x^2(1+x^2)}(x - \arctan(x)). \quad (\text{A.10})$$

This result can be substituted in equation A.8 to obtain:

$$\rho_{\text{iso}}(r)\sigma(r)^2 = 4\pi G \rho_0^2 r_c^2 \int_{r/r_c}^\infty \frac{dx}{x^2(1+x^2)}(x - \arctan(x)), \quad (\text{A.11})$$

$$\rho_{\text{iso}}(r)\sigma(r)^2 = 4\pi G \rho_0^2 r_c^2 \left( \frac{\pi^2}{8} - \frac{1}{2} \arctan^2\left(\frac{r}{r_c}\right) - \frac{r_c}{r} \arctan\left(\frac{r}{r_c}\right) \right). \quad (\text{A.12})$$

This gives a value for  $\sigma(r)^2$ , which can be used in equation 5.16 to find the maximum coarse grained phase space density:

$$F_{\text{cg,iso}}(r) = \rho_{\text{iso}}(r)^{\frac{5}{2}} \left( 8\pi^2 G \rho_0^2 r_c^2 \left( \frac{\pi^2}{8} - \frac{1}{2} \arctan^2\left(\frac{r}{r_c}\right) - \frac{r_c}{r} \arctan\left(\frac{r}{r_c}\right) \right) \right)^{-\frac{3}{2}}. \quad (\text{A.13})$$

This function has a global maximum for  $r = 0$ . The isothermal density profile has a core density of  $\rho_0 = 1.387 \text{ GeV/cm}^3$  and a core radius of  $r_c = 4.38 \text{ kpc}$ [20]. These values at the global maximum give the minimum neutrino mass needed to explain all dark matter:

$$m_\nu \geq \left( \frac{2h^3 F_{\text{cg,iso}}(0)}{g_\nu} \right)^{\frac{1}{4}} = 40.59 \frac{\text{eV}}{c^2}. \quad (\text{A.14})$$

Comparing this result with the result from equation 5.21, we can see that the mass bound is similar for the isothermal and NFW profile. We can again see that the minimum neutrino mass is orders of magnitude larger than the upper limit on the sum of neutrino masses, which shows neutrinos cannot account for all dark matter in a CDDE universe.

## References

- [1] Barbara Ryden. *Introduction to cosmology*. Cambridge University Press, 2017.
- [2] Licia Verde, Tommaso Treu, and Adam G. Riess. Tensions between the early and late universe. *Nature Astronomy*, 3(10):891–895, September 2019.
- [3] Aura Astronomy, Our mysterious universe still evades cosmological understanding. <https://www.aura-astronomy.org/blog/2023/03/06/our-mysterious-universe-still-evades-cosmological-understanding/>. Accessed: 22-12-2023.
- [4] Vito Antonelli and L. Miramonti. Status and potentialities of the juno experiment. March 2018. <https://doi.org/10.22323/1.307.0056>.
- [5] Pavan Kumar Aluri, Paolo Cea, Pravabati Chingambam, Ming-Chung Chu, Roger G Clowes, Damien Hutsemékers, Joby P Kochappan, Alexia M Lopez, Lang Liu, Niels C M Martens, C J A P Martins, Konstantinos Migkas, Eoin Ó Colgáin, Pratyush Pranav, Lior Shamir, Ashok K Singal, M M Sheikh-Jabbari, Jenny Wagner, Shao-Jiang Wang, David L Wiltshire, Shek Yeung, Lu Yin, and Wen Zhao. Is the observable universe consistent with the cosmological principle? *Classical and Quantum Gravity*, 40(9):094001, April 2023.
- [6] N Aghanim *et al.* Planck2018 results: Vi. cosmological parameters. *Astronomy & Astrophysics*, 641:A6, September 2020.
- [7] Rodney Loudon. *The Quantum Theory of Light*. Oxford Science Publications, 3rd edition, 2000.
- [8] R. L. Workman *et al.* Review of Particle Physics. *PTEP*, 2022:083C01, 2022.
- [9] Tijmen Melssen. Photon-Baryon Fluid Physics in a Curvature Dependent Dark Energy Universe, Bachelor’s thesis, Radboud University, November 2023, <https://www.ru.nl/highenergyphysics/theses/bachelor-theses/>.
- [10] Wim Beenakker and David Venhoek. A structured analysis of hubble tension, 2021. <https://doi.org/10.48550/arXiv.2101.01372>.
- [11] R. Rashidi, F. Ahmadi, and M. R. Setare. Particle creation in the framework of  $f(R)$  gravity. *Astrophysics and Space Science*, 363(9), August 2018.
- [12] L. H. Ford. Gravitational particle creation and inflation. *Phys. Rev. D*, 35:2955–2960, May 1987.
- [13] Sabine Hossenfelder, Dominik J Schwarz, and Walter Greiner. Particle production in time-dependent gravitational fields: the expanding mass shell. *Classical and Quantum Gravity*, 20(11):2337–2353, May 2003.

- [14] Thijs van Rossum. Solving the Hubble tension with a curvature dependent dark energy. Master’s thesis, University of Twente, October 2023. <https://www.ru.nl/highenergyphysics/theses/master-theses/>.
- [15] Edvige Corbelli and Paolo Salucci. The extended rotation curve and the dark matter halo of M33. *Monthly Notices of the Royal Astronomical Society*, 311(2):441–447, 01 2000.
- [16] Phys.org Could dark matter not matter? <https://phys.org/news/2011-12-dark.html> Accessed: 31-12-2023.
- [17] Steen H. Hansen. Dark matter density profiles from the jeans equation. *Monthly Notices of the Royal Astronomical Society*, 352(4):L41–L43, August 2004.
- [18] Mark Vogelsberger, Amina Helmi, Volker Springel, Simon D. M. White, Jie Wang, Carlos S. Frenk, Adrian Jenkins, Aaron Ludlow, and Julio F. Navarro. Phase-space structure in the local dark matter distribution and its signature in direct detection experiments. *Monthly Notices of the Royal Astronomical Society*, 395(2):797–811, 04 2009.
- [19] David Merritt, Alister W. Graham, Ben Moore, Jürg Diemand, and Balša Terzić. Empirical models for dark matter halos. i. nonparametric construction of density profiles and comparison with parametric models. *The Astronomical Journal*, 132(6):2685–2700, January 2006.
- [20] Melissa van Beekveld. Possible indirect detection of dark matter and its impact on lhc supersymmetry searches, 2016. <https://www.ru.nl/highenergyphysics/theses/master-theses/>.
- [21] Arthur Loureiro, Andrei Cuceu, Filipe B. Abdalla, Bruno Moraes, Lorne Whiteway, Michael McLeod, Sreekumar T. Balan, Ofer Lahav, Aurélien Benoit-Lévy, Marc Manera, Richard P. Rollins, and Henrique S. Xavier. Upper bound of neutrino masses from combined cosmological observations and particle physics experiments. *Phys. Rev. Lett.*, 123:081301, Aug 2019.
- [22] Malcolm Longair. *Galaxy Formation*. Springer Science & Business Media, 2007.
- [23] Tanisha Joshi and S. D Pathak. Evolution of entropy with cosmic time, 2023. <https://doi.org/10.48550/arXiv.2308.05025>.
- [24] D. Baumann. *Cosmology*. Cambridge University Press, 2022.
- [25] D. J. Fixsen and J. C. Mather. The spectral results of the far-infrared absolute spectrophotometer instrument on COBE, *The Astrophysical Journal*, dec 2002.
- [26] Enrique Gaztañaga. The mass of our observable Universe. *Monthly Notices of the Royal Astronomical Society: Letters*, 521(1):L59–L63, 03 2023.

- [27] P. A. R. Ade *et al.* Planck2013 results. i. overview of products and scientific results. *Astronomy and Astrophysics*, 571:A1, October 2014.
- [28] John Terning Itzhak Bars. *Extra Dimensions in Space and Time*. Springer Science & Business Media, 2009.